Proceedings of the Fifth (1995) International Offshore and Polar Engineering Conference
The Hague, The Netherlands, June 11-16, 1995

ISBN 1-880653-16-8 (Set); ISBN 1-880653-20-6 (Vol IV)

Environmental Description for Long-Term Load Response of Ship Structures

Elzbieta M. Bitner-Gregersen
Det Norske Veritas Research AS, Høvik, Norway

Espen H. Cramer
Det Norske Veritas Industry AS, Høvik, Norway

Florus Korbijn
Det Norske Veritas Classification AS, Høvik, Norway

ABSTRACT

The present study discusses the influence of an adjustment of the *Global Wave Statistics* data for the North Atlantic and world-wide trade on the long-term load response of ship structures. Special emphasis is given to the wave period, where a general procedure for correction of the wave period bias, based on the average wave steepness, is suggested. Using the calibrated wave period, an adjusted scatter diagram for the North Atlantic is proposed. The scatter diagram is numerically generated from a joint distribution combining a marginal 3-parameter Weibull distribution for significant wave height with a conditional log-normal distribution for zero-crossing wave period. An adjusted description of the word-wide environment is also suggested. Numerical examples illustrating the effect of the *Global Wave Statistics* wave period accuracy on the ship load response are given.

KEY WORDS: Wave environment, ship structures, load response

INTRODUCTION

The *Global Wave Statistics* (*GWS*) visual observations of wave climate, Hogben et al. (1986), represent the only truly global set of wave data with a sufficient long observation history to give reliable global climatic statistics. The observations of wave height, period and direction have been reported from ships in normal service all over the world since 1949; wind speeds (Beaufort Scale) and directions and wave heights in a coarse code have been reported since 1854. The observations have been made in accordance with guidance notes prescribed by the World Meteorological Organisation (WMO). The *GWS* data are an important source of statistical information needed for the prediction of design and operational conditions of ocean structures, especially ship structures. The usefulness of these visual observations depends, however, on a proper calibration with accurate measurements of the wave characteristics.

Hogben et al. (1986) compared the *GWS* marginal distributions for wave heights and wave periods with instrumental Shipborne Wave Recorder and NOAA buoy data for different locations and concluded that the wave heights and periods, for which statistics was given, corresponded to measured values. It was stated also that it should not be necessary to apply any correction factors, usually used for estimating significant wave heights from visual wave height observations. Furthermore, it was pointed out by the authors that the *GWS* data covered much longer periods of years than the instrumental data used for the comparison and that the quality of instrumental data could vary quite widely, in particular in estimation of the zero-crossing wave periods. However, the accuracy of the *GWS* data is still questioned in the literature, especially concerning wave period, confer e.g. Guedes Soares and Moan (1991).

Some indication of the accuracy of the *Global Wave Statistics* data was given by Chen and Thayamballi (1991) and Bitner-Gregersen et al. (1993,1994). Chen and Thayamballi (1991) compared the effect of use of the *GWS* data contra hindcast data in ship response analyses. For some ocean zones the *GWS* data led to higher responses and slightly higher fatigue damage. However, this was not necessarily the case for other ocean areas. It was concluded that the two sets of wave data were not quite consistent and should be used with care.

Bitner-Gregersen et al. (1993) compared the *GWS* data with the WRB and ODAP buoy data accepted as the standard wave measurements for design work at sea. For the three locations considered the 20-year extreme values evaluated based on the *GWS* data deviated from the extremes obtained by use of the instrumental data. It was indicated that the *Global Wave Statistics* data may underestimate the zero-crossing wave period, while the data can both underestimate as well as overestimate the significant wave height. This conclusion was also confirmed by the investigations carried out by Bitner-Gregersen and Cramer (1994). For the six locations analysed, the zero-crossing wave period mean value was systematically overestimated for low h_s while it was underestimated for large h_s (except for the North Atlantic where an underestimation of wave period was experienced). The opposite effect was observed for the zero-crossing wave period standard deviation.

In spite of the indicated discrepancies between the *GWS* data and the instrumental measurements Bitner-Gregersen and Cramer (1994) suggested, based on the *GWS* data, scatter diagrams of significant wave height and zero-crossing wave period for North Atlantic and world-wide trade. The scatter diagrams have been primary intended for use in evaluation of ship fatigue damage. It was indicated that the fatigue damage was not very sensitive to a possible inaccuracy of the *GWS* wave period. However, the suggested scatter diagrams can not be uncritically adopted for ultimate limit state calculations of ship structures as the average wave steepness of extre-

me waves, evaluated from the scatter diagrams, is too high.

In the present study a general procedure for correction of the bias of the wave period mean value is suggested. Furthermore, based on the calibrated wave period a standard scatter diagram for the North Atlantic is proposed. The scatter diagram is numerically generated from a joint distribution combining a marginal 3-parameter Weibull distribution for significant wave height with a conditional log-normal distribution for zero-crossing wave period given the significant wave height. An adjusted description of the word-wide environment is also suggested.

Examples of the effect of the North Atlantic and world-wide wave period uncertainty for ship extreme load response are given.

ORIGINAL SCATTER DIAGRAMS

In the *GWS* atlas, Hogben et al. (1986), the ocean areas are divided into 104 regions as shown in Fig. 1.

Based on the *GWS* data two scatter diagrams of H_s and T_z : for the North Atlantic and world-wide trade have been defined, Bitner-Gregersen and Cramer (1994). The North Atlantic scatter diagram has been derived as the average scatter diagram for ocean zone 8, 9 and 15. The scatter diagram for world-wide trade represents the weighted scatter diagram for the following world-wide sailing route: Europe-USA East Coast-USA West Coast-Japan-Persian Gulf-Europe (around Africa).

Both scatter diagrams have been fitted with a joint environmental model combining a marginal 3-parameter Weibull distribution for significant wave height

$$f_{H_s}(h_s) = \frac{\beta}{\alpha}\left[\frac{h_s-\gamma}{\alpha}\right]^{\beta-1} \exp\left[-\left(\frac{h_s-\gamma}{\alpha}\right)\right] \tag{1}$$

with a conditional log-normal distribution for zero-crossing wave period

$$f_{T_z|H_s}(t_z|h_s) = \frac{1}{\sqrt{2\pi}\sigma t_z} \exp\left[\frac{(\ln t_z-\mu)^2}{2\sigma^2}\right] \tag{2}$$

where

$$\mu = \mathrm{E}(\ln T_z) \tag{3}$$

$$\sigma^2 = \mathrm{Var}(\ln T_z) \tag{4}$$

$$\mu = a_o + a_1 h_s^{a_2} \tag{5}$$

$$\sigma = b_o + b_1 e^{b_2 h_s} \tag{6}$$

where α =scale parameter, β =slope parameter, and γ =location parameter.

Table 1 Weibull and log-normal parameters of the joint distribution of H_s and T_z

Sailing Route	H_s Weibull parameters			T_z Log-normal parameters					
				μ			σ		
	α	β	γ	a_o	a_1	a_2	b_o	b_1	b_2
N.Atlantic	2.721	1.401	0.866	0.623	1.339	0.105	0.146	0.044	-1.711
World-wide	1.798	1.214	0.856	-1.010	2.835	0.069	0.161	0.146	-0.683

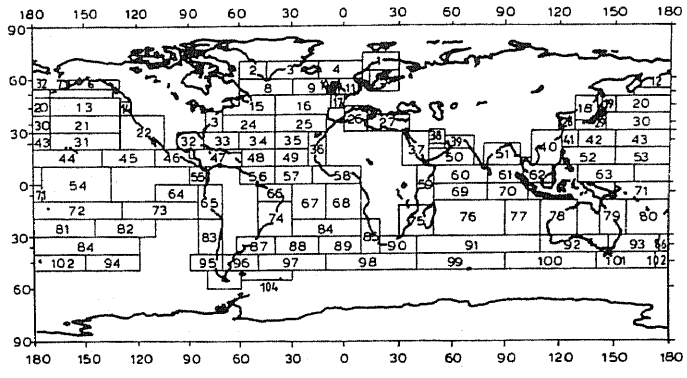

Fig. 1 *Global Wave Statistics* zone designation.

The parameters a_o, a_1, a_2, b_o, b_1 and b_2 are site specific and have been determined from the actual data by the least squared method, see Table 1. It is required when fitting a 3-parameter Weibull distribution to the data to permit some of the observations to lie below the fitted location parameter γ , see Mathisen and Bitner-Gregersen (1990). A threshold level, *thr*, related to choice of the location parameter γ equal to 0.1 has been adopted.

AVERAGE WAVE STEEPNESS

The average wave steepness can be defined as

$$S_t = 2\pi \ H_s / gT_z^2 \tag{7}$$

where H_s denotes significant wave height and T_z zero-crossing wave period (H_{mo} , T_{mo2}, respectively if wave height and period are evaluated from the wave spectrum).

Various studies concerning the average wave steepness have been carried out. In the Haltenbanken Area Metocean Study, HAMS, Bjerke et al. (1990), the following relationships have been suggested for storm conditions

$$T_{mo2} = 3.9 H_{mo}^{0.41} \tag{8}$$

and

$$S_t = 0.042 H_{mo}^{0.18} \tag{9}$$

The expressions (8) and (9) were derived based on measurements collected in the period 1980-1988 at the severe wave climate at Haltenbanken with a Datawell Waverider and a Norwave directional wave buoy. Missing data were replaced with WINCH hindcast data from the Norwegian Meteorological Institute for grid point 1221. The hindcast data were correlated to measured data and adjusted prior to implementation.

The same data base was used by Mathiesen and Torsethaugen (1992) to compute the distribution of average wave steepness for different levels of the significant wave height. The analysis showed that both the standard deviation and the skewness of the average wave steepness decreased to values near zero as the significant wave height increased. For the range of h_{mo} values for which measured data were available, the distributions of wave steepness fitted relatively well to a 3-parameter Weibull distribution, which was adopted to extrapolate the 100-year return period wave steepness. The investigations showed that the average steepness increased with the significant wave height, while the 100-year steepness decreased for increasing wave height. For values of h_{mo} below the 100-year value, the 100-year steepness had a maximum $s_t = 0.10$ for h_{mo} in the middle range $(3-7m)$. For $h_{mo} = 15m$ the steepness was estimated to $s_t = 0.068$ with standard deviation 0.005. The highest measured $h_{mo} = 12.5m$ had wave steepness $s_t = 0.069$.

Wave measurements carried out around Iceland in 1990 showed that h_{mo} around $16.5m$ had the highest wave steepness $s_t = 0.066$, Mathiesen and Torsethaugen (1992).

The DNV Classification Note No. 31.4 (1987) recommends that the sea steepness need not to be taken greater than the 100 year sea steepness for unrestricted service, which normally may be adopted as:

$$s_t = \begin{cases} 1/10 & \text{for} \quad t_z \le 6\,\text{sec} \\ 1/15 & \text{for} \quad t_z \ge 12\,\text{sec} \\ \textit{linear interpolation} & \text{for} \quad 6 < t_z < 12\,\text{sec} \end{cases} \tag{10}$$

$s_t = 1/15 \approx 0.067$ is very close to the wave steepness measured around Iceland and at Haltenbanken.

The average wave steepness of extreme waves evaluated based on the *GWS* scatter diagrams is higher than the measured steepnesses and the steepness recommended by the DNV Classification Note. For the *GWS* North Atlantic scatter diagram (see Table 1)

$$h_{s_{100}} = \gamma + \alpha(\ln N)^{1/\beta} = 17.2m \tag{11}$$

$$\bar{T}_{z|h_{s100}} = \exp(\mu + \frac{1}{2}\sigma^2) = 11.5\,\text{sec} \tag{12}$$

N in Eq.(12) denotes the number of observations during the 100-year period (the visual observations are registered each 4th hour, thus N=219000). From Eqs.(12) and (13) the 100-year steepness $s_t = 0.084$ which is about 25% higher than the steepness measured. For the *GWS* world-wide scatter diagram the 100-year steepness $s_t = 0.076$.

MODIFIED ENVIRONMENTAL DESCRIPTION

Fig. 2 shows nine weather stations in the North Atlantic where waves have been recorded since 1952. Herein the data from Ocean Station Juliett, J, Draper and Whitaker (1965), and from Ocean Station India, I, Draper and Squire (1967), are considered. The data represents 13-year wave records registered by the Shipborne Wave Recorder (SBWR). It was shown by Graham et al. (1978) for three locations on the UK Continental Shelf that on average the SBWR zero-crossing wave period was unbiased as compared to the WRB wave period measurements while the SWBR significant wave heights were on average 8% higher than the ones recorded by WRB.

Table 2 Weibull and log-normal parameters for the joint distribution of H_s and T_z

H_s Weibull parameters			T_z Log-normal parameters					
			μ			σ		
α	β	γ	a_o	a_1	a_2	b_o	b_1	b_2
Ocean Station India, thr=0								
2.991	1.304	0.721	2.164	0.012	1.460	0.101	0.263	-3.593
Ocean Station Juliett, thr=0/0.1								
2.420	1.169	1.258	1.952	0.168	0.499	0.070	0.066	-0.081
GWS Zone 9, thr=0/0.1								
2.857	1.449	0.838	0.835	1.139	0.119	0.140	0.030	-0.958

A comparison between the Ocean Station India data and the *GWS* ocean zone 9 data is given in Fig. 3, while in Fig. 4 the Ocean Station Juliett and the *GWS* ocean zone 9 data are presented. The fitted joint environmental model is also shown in the figures. Both figures indicate that the *GWS* data underestimates the zero-crossing wave period for the ocean zone 9. The model parameters are given in Table 2.

In Fig. 5 the logarithmic mean value and standard deviation of zero-crossing wave period for the *GWS* North Atlantic scatter diagram and Ocean Station Juliett are presented. As seen the *GWS* mean wave period for significant wave height >5.0m is 10-15% lower than the measured period at Ocean Station Juliett.

Herein a general procedure for correction of the *GWS* wave period is suggested. It is assumed that the *GWS* significant wave height is unbiased for the North Atlantic and the world-wide environment. Furthermore, the average wave steepness related to the 100-year significant wave height is adopted to be equal 0.066. The logarithmic wave period mean is adjusted in such a way that the 100-year wave steepness is obtained. The lowest logarithmic wave period mean is kept unchanged.

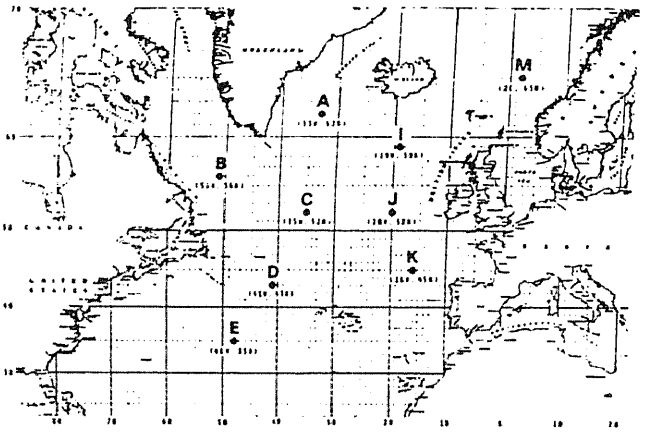

Fig. 2 Locations of nine weather stations in the North Atlantic, Ochi (1978).

For the North Atlantic the adjusted wave period is, see also Fig. 6,

$$\mu = 0.623 + 1.356 h_s^{0.123} \qquad (13)$$

$$\sigma = 0.146 + 0.044 e^{-1.712 h_s} \qquad (14)$$

The wave period described by Eqs.(13) & (14) is close to the period measured at Ocean Station Juliett.

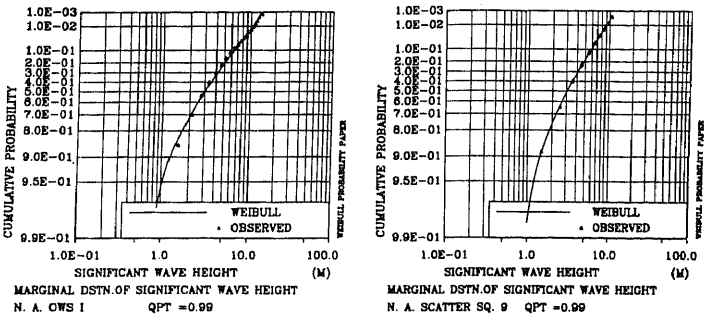

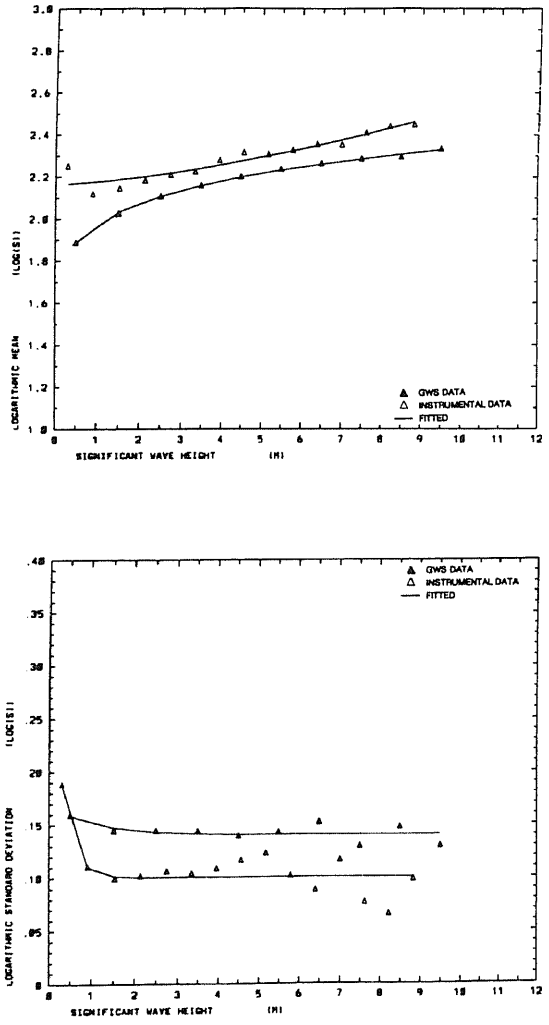

Fig. 3 Comparison between the instrumental (Ocean Station India) and *GWS* (ocean zone 9) marginal distribution of H_s, and conditional mean, μ, and standard deviation, σ, of $\ln T_z$.

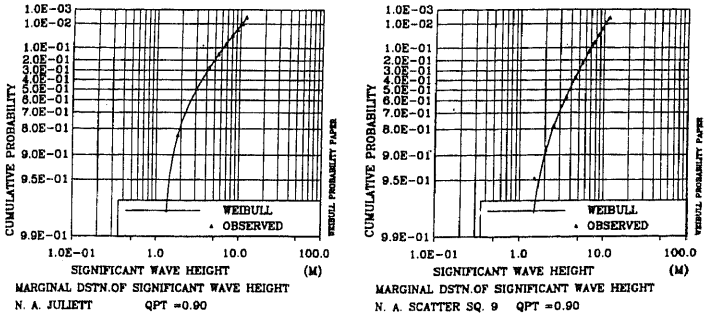

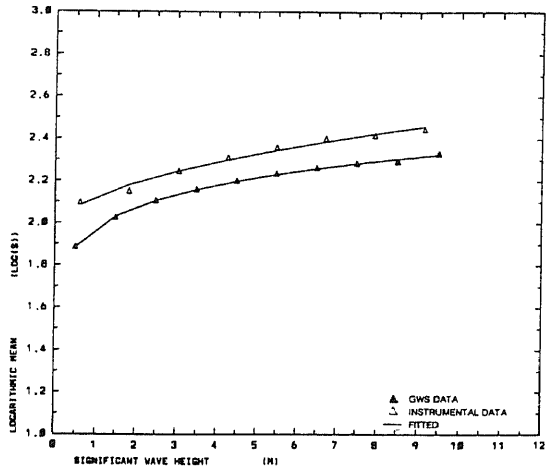

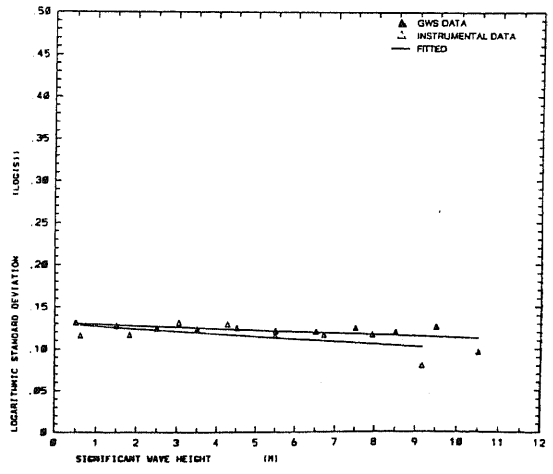

Fig. 4 Comparison between the instrumental (Ocean Station Juliett) and *GWS* (ocean zone 9) marginal distribution of H_s , and conditional mean, μ , and standard deviation, σ , of $\ln T_z$.

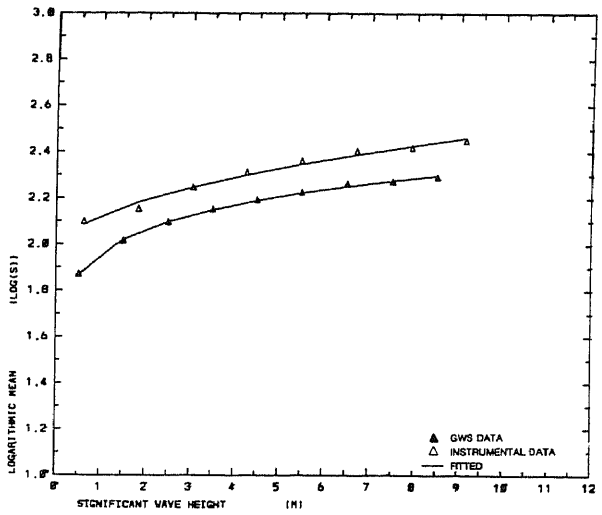

Fig. 5 Comparison between the instrumental (Ocean Station Juliett) and *GWS* North Atlantic scatter diagram conditional mean, μ , and standard deviation, σ , of $\ln T_z$.

Based on the calibrated wave period a scatter diagram for the North Atlantic is proposed, see Table 3. The diagram is numerically generated from the joint environmental model, see Eqs.(1)-(6) and Table 1.

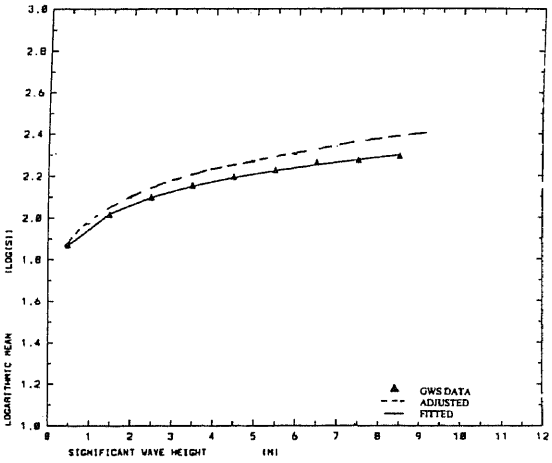

Fig. 6 Adjusted logarithmic mean value of T_z for the North Atlantic.

Applying the same correction procedure as described above the adjusted world-wide wave period is, see also Figure 7,

$$\mu = -1.010 + 2.847 h_s^{0.075} \tag{15}$$

$$\sigma = 0.161 + 0.146 e^{-0.683 h_s} \tag{16}$$

Table 3 Scatter diagram for the North Atlantic, $\sum 100000$.

tz	3.5	4.5	5.5	6.5	7.5	8.5	9.5	10.5	11.5	12.5	13.5	14.5	15.5	16.5	17.5	18.5
hs																
1.0	0	73	1416	4594	4937	2590	839	195	36	6	1	0	0	0	0	0
2.0	0	5	356	3299	8001	8022	4393	1571	414	87	16	3	0	0	0	0
3.0	0	0	62	1084	4428	6920	5566	2791	993	274	63	12	2	0	0	0
4.0	0	0	12	318	1898	4126	4440	2889	1301	445	124	30	6	1	0	0
5.0	0	0	2	89	721	2039	2772	2225	1212	494	162	45	11	2	1	0
6.0	0	0	1	25	254	896	1482	1418	907	428	160	50	14	3	1	0
7.0	0	0	0	7	85	363	710	791	580	311	131	46	14	4	1	0
8.0	0	0	0	2	27	138	312	398	330	197	92	35	12	3	1	0
9.0	0	0	0	1	8	50	128	184	171	113	58	24	9	3	1	0
10.0	0	0	0	0	3	17	50	80	82	59	33	15	6	2	1	0
11.0	0	0	0	0	1	6	18	33	37	29	17	8	3	1	0	0
12.0	0	0	0	0	0	2	7	13	15	13	8	4	2	1	0	0
13.0	0	0	0	0	0	1	2	5	6	6	4	2	1	0	0	0
14.0	0	0	0	0	0	0	1	2	2	2	2	1	1	0	0	0
15.0	0	0	0	0	0	0	0	1	1	1	1	0	0	0	0	0
16.0	0	0	0	0	0	0	0	0	0	0	0	0	0	0	0	0

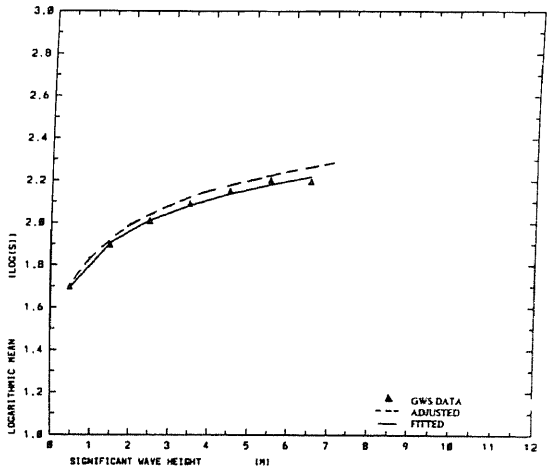

Fig. 7 Adjusted logarithmic mean value of T_z for the world-wide environment.

NUMERICAL EXAMPLES

In order to study the influence of the *GWS* wave period bias on the wave induced extreme load characteristics three ships, are considered: an oil tanker, a container vessel and a bulk ship. The ships characteristics are given in Table 4

Table 4 Ship characteristics

Ship type	Block coefficient C_B	Ship lenght L (m)	Ship width B (m)
Tanker	0.85	250.0	40.0
Container vessel	0.64	309.0	38.0
Bulk ship	0.81	185.0	30.5

For the tanker the long-term cumulative distribution of the stress amplitude is evaluated assuming a linear model and narrow-banded response

$$F_{s_a}(s_a)_{long-term} = \sum_{i=1}^{n} \iint \bar{\nu}(h_s,t_z) F_{s_a}(s_a|h_s t_z) f(h_s,t_z)_i dh_s dt_z p_i \qquad (17)$$

where $F_{s_a}(s_a|h_s,t_z)$ is the short-term Rayleigh distributed response function, $\bar{\nu}(h_s,t_z)$ is the relative rate of wave cycles within each sea state, p_i denotes the frequency of occurrence of the ship in nautical area i ($i=1,...,104$; see Fig. 1), and n is the number of nautical areas considered. A Monte Carlo simulation technique is used to solve the integrals in Eq.(17). Furthermore, the long-term stress amplitude distribution is approximated by a two-parameter Weibull distribution

$$F_{s_a}(s_a)_{long-term} = 1 - \exp\left[-(s_a / A)^B\right] \qquad (18)$$

where A and B are the scale and shape parameter, respectively.

Based on the determined long-term stress distribution, the most probable 1-year and 20-year extreme values for the original and adjusted joint environmental models are estimated, see Table 5. The long-term stress distributions for the North Atlantic and world-wide environment are shown in Fig. 8 and 9, respectively.

Table 5 Extreme stress amplitude for the tanker

Ocean area	A	B	1-year ext. stress (MPa)	20-year ext. stress (MPa)
GWS N. Atlantic	8.88	1.03	121.2	144.6
Adjusted N.Atlantic	8.02	0.99	124.3	149.4
GWS World-wide	4.94	0.89	104.6	128.1
Adjusted W.-wide	5.35	0.92	103.1	125.4

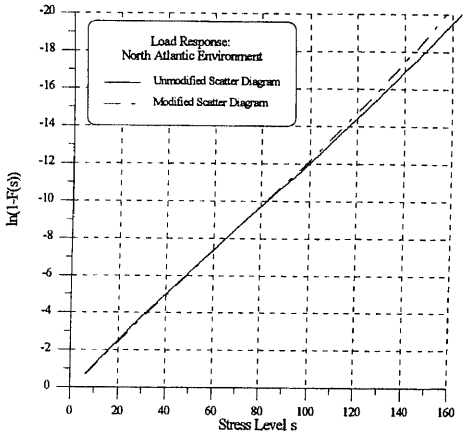

Fig. 8 Long-term stress distributions for the North Atlantic environment.

As seen in Table 5 for the tanker considered, the stress extremes are found not to be very sensitive to the wave period bias.

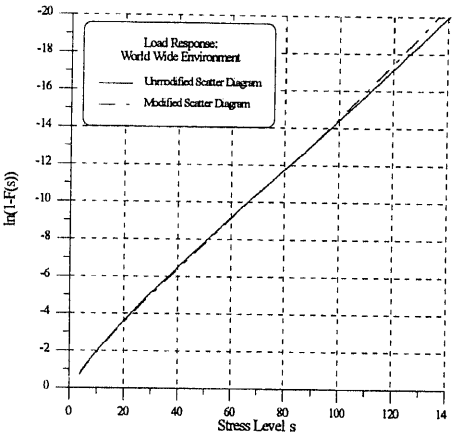

Fig. 9 Long-term stress distributions for the world-wide environment.

Table 6 includes the load characteristics for a container vessel and a bulk carrier estimated by strip theory, Veritas Sesam Systems (1989). For both ships the inaccuracy of the *GWS* wave period have some influence on the load responses which are increased up to 7.0% when the adjusted scatter diagram is applied.

Table 6 20-year extreme ship load characteristics

Ship type	Scatter diagram	Midship vertical bending moment (kNm)	Torsional moment in shear centre (kNm)
Container ves.	*GWS* N. A.	$6.87 \cdot 10^6$	$1.15 \cdot 10^6$
Container ves.	Adjusted N. A.	$7.35 \cdot 10^6$	$1.22 \cdot 10^6$
Bulk carrier	*GWS* N. A.	$1.58 \cdot 10^6$	$3.70 \cdot 10^6$
Bulk carrier	Adjusted N. A.	$1.69 \cdot 10^6$	$3.96 \cdot 10^6$

CONCLUSIONS

The *Global Wave Statistics* data are fitted with a joint distribution combining a 3-parameter Weibull distribution for significant wave height with a conditional log-normal distribution for zero-crossing wave period. The study indicates that the 100-year average wave steepness evaluated based on the *Global Wave Statistics* North Atlantic and world-wide environment is too high as compared to some measured values and the value recommended by the DNV Classification Note. An adjustment of the data for use in long-term ship response analyses is suggested. The numerical examples presented suggest that the ship load characteristics can be influenced by a possible inaccuracy of the *GWS* wave period.

ACKNOWLEDGEMENTS

This study has been carried out under the strategic research program PROCLASS at Det Norske Veritas. The company financial support and permission to publish the results are gratefully acknowledged. The opinions expressed herein are those of authors and should not be construed as reflecting the views of the company.

REFERENCES

Bitner-Gregersen, E.M. Cramer, E.H. and Løseth, R., "Uncertainty of Load Characteristics and Fatigue Damage of Ship Structures", Marine Structure Journal, Vol.8, 1995.

Bitner-Gregersen, E.M. and Cramer, E.H. "Accuracy of the Global Wave Statistics Data", Proceedings of the ISOPE-94 conference, Osaka 1994.

Bjerke, P.L., Mathiesen, M., Torsethaugen, K. (1990), "Haltenbanken Area Metocean Study", Main Report SINTEF NHL 1990, STF60 A90055.

British Maritime Technology (Primary Contributors Hogben, N., Da Cunha, L.F. and Olliver, H.N.) "Global Wave Statistics", Unwin Brothers Limited, London 1986.

Chen, Y.R.N. and Thayamballi, A.K., "Consideration of Global Climatology and Loading Characteristics in Fatigue Damage Assessment of Ship Structures", The Marine Structural Inspection, Maintenance, and Monitoring Symposium, Virginia, March, 1991.

DNV Classification Note No.31.4, "Column Stabilized Units (Semisubmersible Platforms)", September 1987.

Mathisen, J., and Bitner-Gregersen, E.M., " Joint Distributions for Significant Wave Height and Wave Zero-Crossing Period", Applied Ocean Research, Vol. 12, No. 2, April 1990.

Mathiesen, M. and Torsethaugen, K., "Some Aspects of the Wave Climate at the Draugen Field", SINTEF NHL Report No.STF60 F92087, October 1992.

Guedes Soares, C., and Moan, T. "Model Uncertainty in the Long-term Distribution of Wave-induced Bending Moments for Fatigue Design of Ship Structures", Marine Structures, Vol.4, 1991.

Veritas Sesam System, "Sesam POSTRESP , User's Manual" , December, 1989.